Journal of Applied Sciences

ISSN 1812-5654

science alert

ANSInet
an open access publisher
http://ansinet.com

Journal of Applied Sciences 9 (5): 962-967, 2009
ISSN 1812-5654

Numerical Analysis of Bio-Heat Transfer in a Spherical Tissue

Po-Jen Cheng and Kuo-Chi Liu
Department of Mechanical Engineering, Far East University, 49 Chung Hua Road,
Hsin-Shih, Tainan 744, Taiwan

Abstract: This study uses the Pennes bioheat equation in spherical co-ordinates to describe the heat transport occurring in biological tissues during magnetic tumor hyperthermia. A hybrid numerical scheme based on the Laplace transform, change of variables and the modified discretization technique in conjunction with the hyperbolic shape functions is proposed for solving the present problem. The effects of blood perfusion, metabolism and the difference of thermophysical properties between the diseased and health tissues are explored. The accuracy of the numerical results is evidenced by comparing with the results in the literature. The metabolic heat generation rate and the blood perfusion rate practically affect the temperature rise behavior *in vivo* during hyperthermia treatment.

Key words: Hyperthermia, Laplace transform, modified discretization technique, Pennes bioheat equation, perfused tissue

INTRODUCTION

Hyperthermia uses the physical methods to heat certain organ or tissue to the temperatures in the range of 40-44°C with treatment times over 30 min. In general, cancer cells have a higher chance of dying when the temperature is above 42.5°C and the rate of death drastically increases with increasing temperature (Moroz *et al*., 2002). An ideal hyperthermia treatment should selectively destroy the tumor cells without damaging the surrounding healthy tissue. Magnetic fluid hyperthermia is one of hyperthermia modalities for tumor treatment. It is absolutely a necessity to understand the temperature rise behavior occurring in biological tissues during treatment. Especially, the temperature distribution inside as well as outside the target region must be known as function of the exposure time in order to provide a level of therapeutic temperature and on the other hand, to avoid overheating and damaging of the surrounding healthy tissue.

Andrä *et al*. (1999), Bagaria and Johnson (2005) and Maenosono and Saita (2006) studying magnetic fluid hyperthermia used the Pennes' equation to describe the behavior of heat transfer in biological tissues. Andrä *et al*. (1999) modeled small breast carcinomas surrounded by extended health tissue as a solid sphere with constant heat generation and gave an elementary solution of the original heat conduction problem without the effects of blood perfusion and metabolism. Bagaria and Johnson (2005) considered the tissue model as two finite concentric spherical regions with the blood perfusion effect. Analytical and numerical solutions to the model with the mixed boundary conditions were calculated by separation of variables and an explicit finite differencing technique, respectively. Maenosono and Saita (2006) carried out theoretical assessment of FePt magnetic nanoparticles as heating elements for hyperthermia using the heat generation model and the bioheat transfer equation. To estimate the temperature rise behavior *in vivo*, the Pennes bioheat equation with the Neuman boundary conditions in spherical co-ordinates was solved with the same thermal properties in the diseased and healthy tissues. Durkee *et al*. (1990) also gave the exact solutions to the Pennes bioheat equation in one-dimensional multi-layer spherical geometry. Tsuda *et al*. (1996) developed an inverse method to optimize the heating conditions during a hyperthermia treatment.

The present study models the tissues within magnetic fluid hyperthermia as an infinite concentric spherical domain. Several methods for solving the heat conduction problems in multi-layer spherical structures have also been developed by Virseda and Pinazo (1998), Chen *et al*. (2003) and Shirmohammadi (2008). This study would develop a hybrid numerical scheme based on the Laplace transform, change of variables and the modified discretization technique in conjunction with the hyperbolic shape functions for solving the present problem. In reality, there exists the difference in metabolic heat generation rate, blood perfusion rate and other

Corresponding Author: Kuo-Chi Liu, Department of Mechanical Engineering, Far East University, 49 Chung Hua Road, Hsin-Shih, Tainan 744, Taiwan

physiological parameters between tumor and normal tissues (Hu *et al*., 2004; Gonźalez, 2007). For complete analysis, this study explores the effects of those differences on the thermal response.

MATHEMATICAL FORMULATION

In magnetic fluid hyperthermia, fine magnetic particles are localized at the tumor tissue. An alternating magnetic field is then applied to the target region, which heats the magnetic particles by magnetic hysteresis losses. These particles might act as localized heat sources. A small tumor surrounded by the normal tissue was modeled as a sphere of the radius R (Andrä *et al*., 1999; Bagaria and Johnson, 2005; Maenosono and Saita, 2006). As magnetic particles are injected into and homogenously distributed in the tumor, a spherical heat source of constant power density P is excited by an alternating magnetic field. Afterward, heat symmetrically transfers in the radius direction. The temperature distribution in the tumor and normal tissues is the function of distance r from the center of the sphere and time t. This system can be mathematically described in the temperature domain as (Andrä *et al*., 1999):

$$\rho_1 c_1 \frac{\partial T_1}{\partial t} = k_1 \frac{1}{r^2}\frac{\partial}{\partial r}(r^2 \frac{\partial T_1}{\partial r}) + w_{b1}\rho_b c_b (T_b - T_1) + q_{m1} + P \quad \text{for } 0 \le r \le R \tag{1}$$

$$\rho_2 c_2 \frac{\partial T_2}{\partial t} = k_2 \frac{1}{r^2}\frac{\partial}{\partial r}(r^2 \frac{\partial T_2}{\partial r}) + w_{b2}\rho_b c_b (T_b - T_2) + q_{m2} \quad \text{for } R \le r \le \infty \tag{2}$$

with the boundary conditions:

$$\frac{\partial T_1(0,t)}{\partial r} = 0 \text{ and } T_1(0,t) \text{ is finite} \tag{3}$$

$$T_1(R,t) = T_2(R,t) \tag{4}$$

$$k_1 \frac{\partial T_1(R,t)}{\partial r} = k_2 \frac{\partial T_2(R,t)}{\partial r} \tag{5}$$

$$T_2(\infty,t) = T_0 \tag{6}$$

and the initial conditions:

$$T_j(r,0) = T_0,\ \frac{\partial T_j(r,0)}{\partial t} = 0 \text{ and } q_j(r,0) = 0 \quad j = 1,\ 2 \tag{7}$$

Here, ρ, c, k and T denote density, specific heat, thermal conductivity and temperature in two regions. ρ_b, c_b and w_b are, respectively, the density, specific heat and perfusion rate of blood. q_m is the metabolic heat generation. T_b is the arterial temperature and was specified as 37°C. The initial temperature T_0 is regarded as the arterial temperature.

Numerical scheme: The present problem is transformed into a problem in the rectangular coordinate system with change of variable. A new dependent variable θ is defined as:

$$\theta = r(T - T_0) \tag{8}$$

Therefore, Eq. 1 and 2 can be written in terms of θ, respectively, as:

$$\rho_1 c_1 \frac{\partial \theta_1}{\partial t} + w_{b1}\rho_b c_b \theta_1 = k_1 \frac{\partial^2 \theta_1}{\partial r^2} + [w_{b1}\rho_b c_b (T_b - T_0) + q_{m1} + P]r \quad \text{for } 0 \le r \le R \tag{9}$$

$$\rho_2 c_2 \frac{\partial \theta_2}{\partial t} + w_{b2}\rho_b c_b \theta_2 = k_2 \frac{\partial^2 \theta_2}{\partial r^2} + [w_{b2}\rho_b c_b (T_b - T_0) + q_{m2}]r \quad \text{for } R \le r \le \infty \tag{10}$$

The boundary condition at r = 0 can be stated from the definition of θ (r,t) shown in Eq. 8 as:

$$\theta_1(0,t) = 0 \tag{11}$$

The other boundary conditions become to:

$$\theta_1(R,t) = \theta_2(R,t) \tag{12}$$

$$k_1(\frac{\partial \theta_1(R,t)}{\partial r} - \frac{\theta_1}{R}) = k_2(\frac{\partial \theta_2(R,t)}{\partial r} - \frac{\theta_2}{R}) \tag{13}$$

$$\theta_2(\infty,t) = 0 \tag{14}$$

The initial conditions are also rewritten as:

$$\theta_j(r,0) = 0,\ \frac{\partial \theta_j(r,0)}{\partial t} = 0 \text{ and } q_j(r,0) = 0 \qquad j = 1,\ 2 \tag{15}$$

And then, using the Laplace transform technique simplifies the transient problem into the steady one. The differential Eq. 9 and 10 and the boundary conditions Eq. 11-14 of the present problem are rewritten as:

$$\frac{d^2\tilde{\theta}_j}{dr^2} - \lambda_j^2 = -f_j r \qquad j = 1,2 \tag{16}$$

and

$$\tilde{\theta}_1(0,s) = 0 \tag{17}$$

$$\tilde{\theta}_1(R,s) = \tilde{\theta}_2(R,s) \tag{18}$$

$$k_1\left(\frac{d\tilde{\theta}_1(R,s)}{dr} - \frac{\tilde{\theta}_1}{R}\right) = k_2\left(\frac{d\tilde{\theta}_2(R,s)}{dr} - \frac{\tilde{\theta}_2}{R}\right) \tag{19}$$

$$\tilde{\theta}_2(\infty,s) = 0 \tag{20}$$

Where:

$$\lambda_j^2 = \frac{1}{k_j}(\rho_j c_j s + w_b \rho_b c_b) \qquad j = 1,2 \tag{21}$$

$$f_1 = \frac{q_{m1} + P}{k_1 s} \tag{22a}$$

$$f_2 = \frac{q_{m2}}{k_2 s} \tag{22b}$$

and s is the Laplace transform parameter for time t.

It is found from Eq. 16 that the governing equations of the present problem have become ordinary differential equations. Their analytical solutions in the sub-space domain k, $[r_i, r_{i+1}]$, with the boundary conditions:

$$\tilde{\theta}_{k,j}(r_i) = \tilde{\theta}_{i,j} \text{ and } \tilde{\theta}_{k,j}(r_{i+1}) = \tilde{\theta}_{i+1,j} \quad i = 1,2,...,n\ ;\ j = 1,2;\ k = i \tag{23}$$

are easily obtained and can be written as:

$$\tilde{\theta}_{k,j} = \frac{1}{\sinh\lambda_j}\left\{(\tilde{\theta}_{i,j} - \frac{f_j}{\lambda_j^2} r_i)\sinh\lambda_j(r_{i+1} - r) + (\tilde{\theta}_{i+1,j} - \frac{f_j}{\lambda_j^2} r_{i+1})\sinh\lambda_j(r - r_i)\right\} + \frac{f_j}{\lambda_j^2} r \tag{24}$$

Similarly, Eq. 24 in the sub-space domain k-1, $[r_{i-1}, r_i]$, can be written as:

$$\tilde{\theta}_{k-1,j} = \frac{1}{\sinh\lambda_j}\left\{(\tilde{\theta}_{i-1,j} - \frac{f_j}{\lambda_j^2} r_{i-1})\sinh\lambda_j(r_i - r) + (\tilde{\theta}_{i,j} - \frac{f_j}{\lambda_j^2} r_i)\sinh\lambda_j(r - r_{i-1})\right\} + \frac{f_j}{\lambda_j^2} r \tag{25}$$

where, *l* denotes the length of sub-space domain or the distance between two neighboring nodes. The value of *l* can be different in the different layer. The subscript i is the number of node. N is the total number of node. A modified discretization technique based on Eq. 24 and 25 is developed for the governing algebraic equations in the present study. The earlier studies have used the similar approximation functions to discretize the hyperbolic and dual-lag-phase diffusion equations (Liu, 2007a, b, 2008).

For continuities of temperature and heat flux within the whole space domain, the following conditions can be required:

$$\tilde{\theta}_{k-1,j}(r_i) = \tilde{\theta}_{k,j}(r_i) \tag{26}$$

$$k_j\left(\frac{d\tilde{\theta}_{k-1,j}(r_i)}{dr} - \frac{\tilde{\theta}_{k-1,j}}{r_i}\right) = k_j\left(\frac{d\tilde{\theta}_{k,j}(r_i)}{dr} - \frac{\tilde{\theta}_{k,j}}{r_i}\right) \tag{27}$$

Substituting Eq. 24, 25 and 26 into Eq. 27 and then evaluating the resulting derivative can lead to the discretized form for the interior nodes in layer j as following:

$$\tilde{\theta}_{i-1,j} - 2\cosh(\lambda_j r)\tilde{\theta}_{i,j} + \tilde{\theta}_{i+1,j} = \frac{f_j}{\lambda_j^2}[r_{i-1} - 2r_i\cosh(\lambda_j r) + r_{i+1}] \tag{28}$$

The discretized form for the node at the interface of the tumor and normal tissues, r = R, can be obtained from the boundary condition Eq. 19 and is written as:

$$\begin{aligned} &k_1\frac{\lambda_1}{\sinh\lambda_1\ell}\tilde{\theta}_{i-1,1} - (k_1\frac{\lambda_1\cosh\lambda_1\ell}{\sinh\lambda_1\ell} + k_2\frac{\lambda_2\cosh\lambda_2\ell}{\sinh\lambda_2\ell} + \frac{k_2}{R} - \frac{k_1}{R})\tilde{\theta}_{i,(1,2)} \\ &+k_2\frac{\lambda_2}{\sinh\lambda_2\ell}\tilde{\theta}_{i+1,2} = k_1\frac{1}{\sinh\lambda_1\ell}\frac{f_1}{\lambda_1}(R-\ell) - (k_1\frac{\cosh\lambda_1\ell}{\sinh\lambda_1\ell}\frac{f_1}{\lambda_1} \\ &+k_2\frac{\cosh\lambda_2\ell}{\sinh\lambda_2\ell}\frac{f_2}{\lambda_2})R + k_2\frac{1}{\sinh\lambda_2\ell}\frac{f_2}{\lambda_2}(R+\ell) + k_1\frac{f_1}{\lambda_1^2} - k_2\frac{f_2}{\lambda_2^2} \end{aligned} \tag{29}$$

Equation 28 and 29 in conjunction with the discretized forms of the boundary conditions can be rearranged as the following matrix equation:

$$[B]\{\tilde{\theta}\} = \{F\} \tag{30}$$

where, [B] is a matrix with complex numbers, $\{\tilde{\theta}\}$ is a column vector in the Laplace transform domain and {F} is a column vector representing the forcing term. Thereafter, the value of H in the physical domain can be determined with the application of the Gaussian elimination algorithm and the numerical inversion of the Laplace transform (Honig and Hirdes, 1984). At the same time, the temperature difference, $T-T_0$, is equal to θ/r. However, the value of θ/r at r = 0 is indeterminate and must be replaced by its limit as $r \to 0$. Thus, the value of the transient temperature at the center, T (0, t), can be evaluated by using L'Hôspital's rule.

RESULTS AND DISCUSSION

Andrä *et al*. (1999) have numerically simulated the thermal behavior of localized magnetic hyperthermia applied to a breast carcinoma and estimated the minimum

amount of iron oxide for getting predetermined temperatures. They considered a small spherical tumor of radius R = 0.00315 m with a constant power density of 6.15×10^6 W m^{-3} embedded in extended muscle tissue. The thermal parameters were taken to be $k_1 = 0.778$, W K^{-1} m, $\rho_1 = 1660$ kg m^{-3}, $c_1 = 2540$ J kg^{-1} K, $k_2 = 0.642$, W K^{-1} m, $\rho_2 = 1000$ kg m^{-3} and $c_2 = 3720$ J kg^{-1} K. For low blood perfusion in breast, Andrä *et al*. (1999) calculated the temperature distribution with neglecting the effects of blood perfusion and metabolism. However, in accordance with the contents of the literatures (Hu *et al*., 2004; Gonźalez, 2007), there exists an obvious difference in metabolic heat generation rate and blood perfusion rate between tumor and normal tissue. This difference may significantly affect the temperature rise during a hyperthermia treatment. Thus, it is explored in the present study. All the computations are performed with the uniform space size l = R/100.

To evidence the accuracy of the present results, the comparison of the present results with those given by Andrä *et al*. (1999) is made, as shown in Fig. 1 and 2. It is found from these two figures that the present results agree well with the results presented in the literature (Andrä *et al*., 1999). This phenomenon demonstrates the efficiency of the present numerical scheme for solving such a problem. Due to continuous heating, temperature at different reduced distance r/R from the center increases with time, as plotted in Fig. 1. On the other hand, heat energy continuously diffuse away in the infinite domain, so the increasing rate of temperature at a specified location decays with time increasing. Figure 2 presents the distributions of temperature increase $T-T_0$ for various times. It is observed that the temperatures in the domain occupied by the heat source get higher and the affected domain increases with time. For an ideal hyperthermia treatment, that should selectively destroy the tumor cells without damaging the surrounding healthy tissue, it is well known the control of exposure time is a necessity.

The metabolic heat generation rates and the blood perfusion rates of tumor and normal tissue in female breast were estimated. Accordingly, Hu *et al*. (2004) took the metabolic heat generation rates of tumor and normal tissue to be $q_{m1} = 29{,}000$ W m^{-3} and $q_{m2} = 450$ W m^{-3} and the corresponding perfusion rates were $w_{b1} = 0.009$ $m^3/s/m^3$ and $w_{b2} = 0.0018$ $m^3/s/m^3$. The product of density and specific heat capacity of blood, $\rho_b c_b = 4.18\times106$ J/m^3/K (Maenosono and Saita, 2006) and the above data are used to investigate the effects of the metabolic heat generation rate and the blood perfusion rate on the temperature rise in the present study. Figure 3 displays the transient temperature rises with and without the effects of the metabolic heat generation rate and the blood perfusion rate at the locations x = 0 and x = R. It can be observed in this case that the effects of the metabolic heat generation rate and the blood perfusion rate make the temperature rise up. However, the blood perfusion plays the cooling role for that the temperature of blood is specified as a constant value, 37°C. In other words, it is the metabolic heat generation to cause the temperature increase in tissues. Judging from this, only using constant power density is not easy to have a constant predetermined tumor temperature during a hyperthermia treatment.

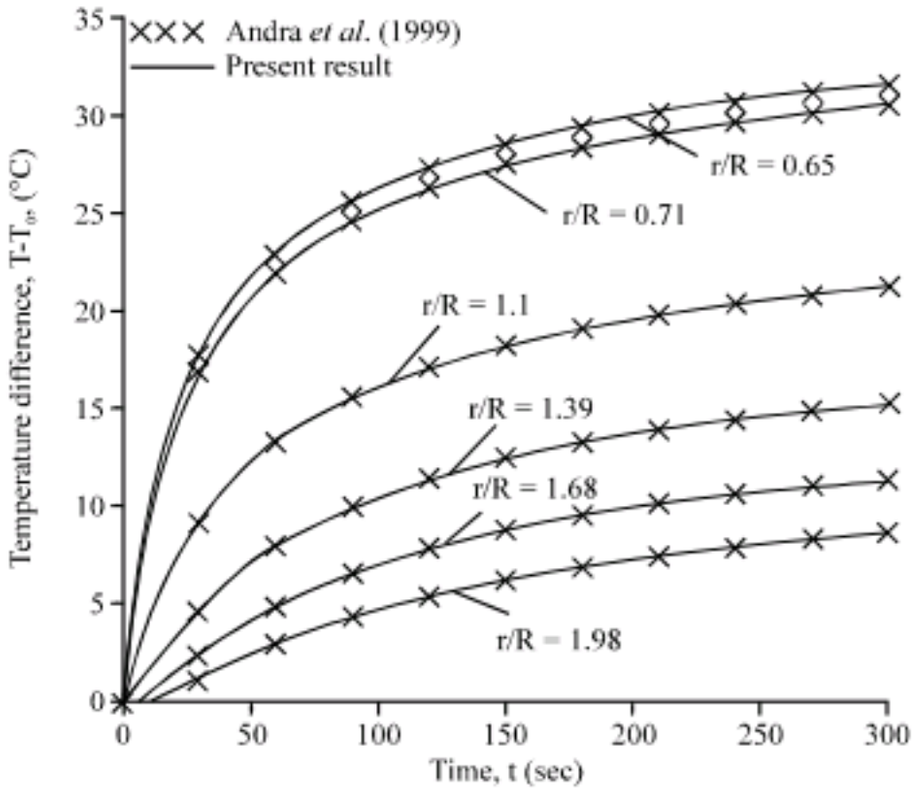

Fig. 1: History of temperature at different reduced distance r/R from the center for the problem in infinite domain

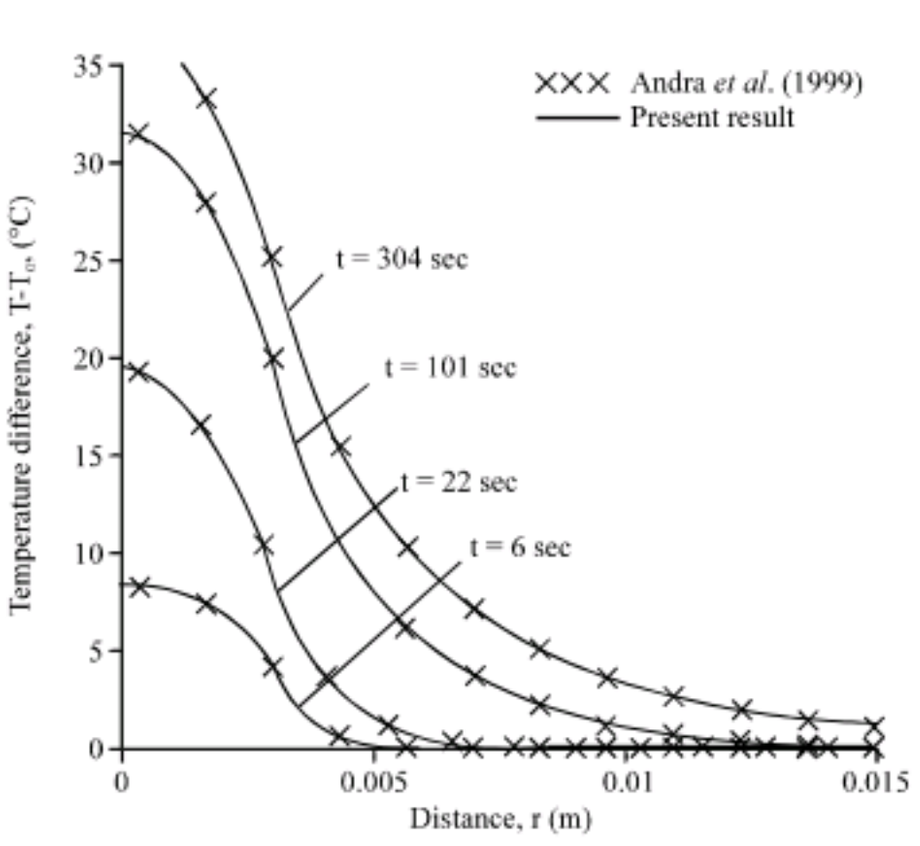

Fig. 2: Temperature distributions in the infinite domain for various times

Figure 4 shows the temperature distributions with metabolism and with blood perfusion and metabolism for various times. The cooling function of blood perfusion is obviously displayed in Fig. 4. Before t = 6 sec the difference between the tumor temperature and the blood temperature is not large enough, so the amount of heat transfer through the blood perfusion is few and the cooling function does not develop yet. With time passing, the accumulation of heat in tissues increases and the tissue temperatures rise up. As the difference between the tissue and blood temperatures is enlarged, the heat loss through

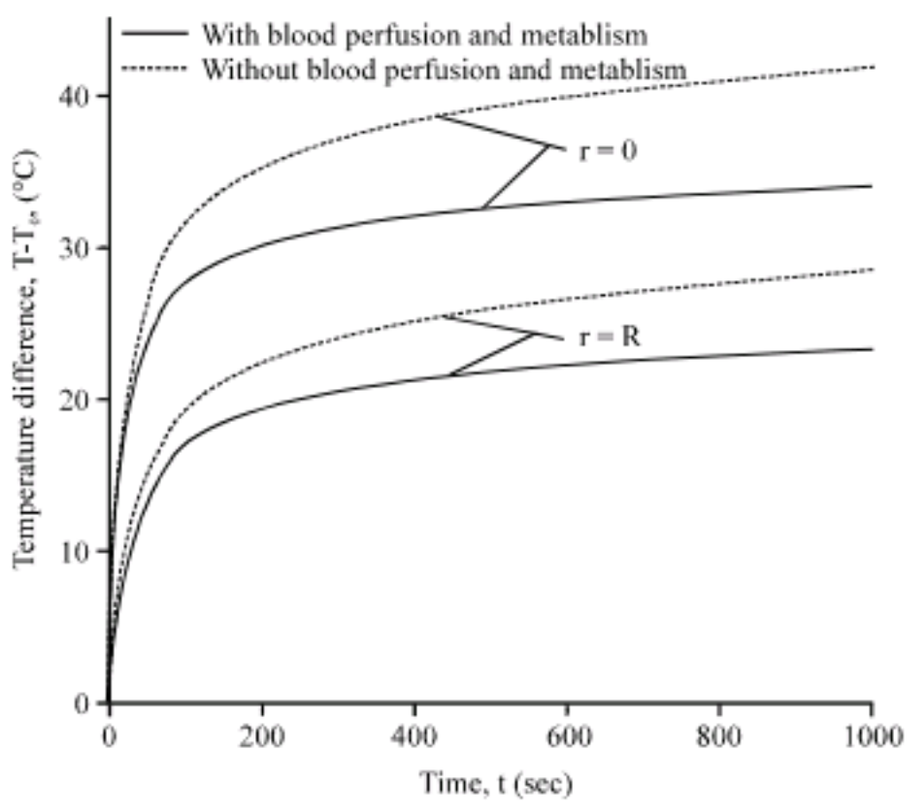

Fig. 3: Variation of temperature rise with and without the effects of the metabolic heat generation rate and the blood perfusion rate at the locations x = 0 and x = R

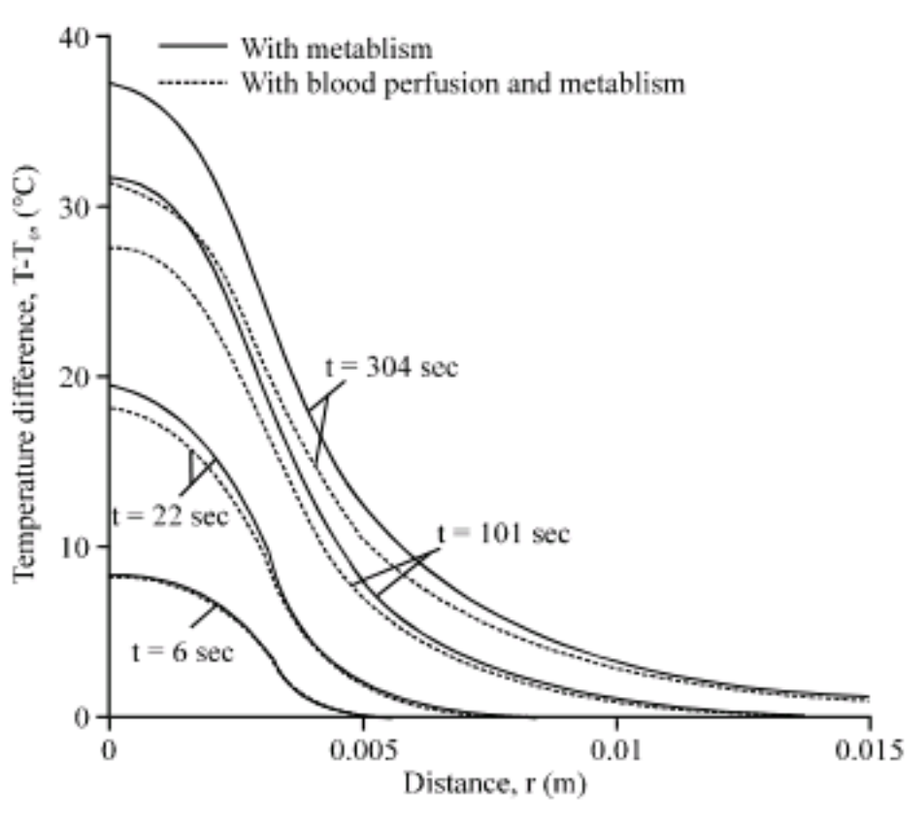

Fig. 4: Effects of blood perfusion on the temperature distributions at various times

the blood perfusion increases. Then the rate of temperature rise tends to be gradual. Probably, the thermal balance will appear for the cooling effect of blood perfusion and the temperature distribution will be steady in the tissues.

CONCLUSION

A hybrid numerical scheme based on the Laplace transform, change of variables and the modified discretization technique in conjunction with the hyperbolic shape functions is developed to solve the Pennes bioheat equation in one-dimensional multi-layer spherical geometry and explores the effects of the difference in metabolic heat generation rate, blood perfusion rate and other physiological parameters between tumor and normal tissues on the thermal response. The accuracy of the numerical scheme is evidenced by comparing with the analytical solution and the results in the literature (Andrä *et al*., 1999). The metabolic heat generation rate and the blood perfusion rate practically affect the temperature rise behavior *in vivo* during hyperthermia treatment. The temperature distribution in tissues can reach the equilibrium state for the cooling effect of blood perfusion.

REFERENCES

Andrä, W., C.G. d'Ambly, R. Hergt, I. Hilger and W.A. Kaiser, 1999. Temperature distribution as function of time around a small spherical heat source of local magnetic hyperthermia. J. Magn. Magn. Mater., 194: 197-203.

Bagaria, H.G. and D.T. Johnson, 2005. Transient solution to the bioheat equation and optimization for magnetic fluid hyperthermia treatment. Int. J. Hyperthermia, 21: 57-75.

Chen, Y., S. Wang and Z. Zuo, 2003. An approach to calculate transient heat flow through multilayer spherical structures. Int. J. Thermal Sci., 42: 805-812.

Durkee, J.W., P.P. Antich and C.E. Lee, 1990. Exact solutions to the multiregion time-dependent bioheat equation. I: Solution development. Phys. Med. Biol., 35: 847-867.

Gonz´alez, F.J., 2007. Thermal simulation of breast tumors. Revista Mexicana de F´isica, 53: 323-326.

Honig, G. and U. Hirdes, 1984. A method for the numerical inversion of Laplace transforms. J. Comp. Applied Math., 10: 113-132.

Hu, L., A. Gupta, J.P. Gore and L.X. Xu, 2004. Effect of forced convection on the skin thermal expression of breast cancer. J. Heat Transfer, 126: 204-211.

Liu, K.C., 2007a. Analysis of thermal behavior in multi-layer metal thin-films based on hyperbolic two-step model. Int. J. Heat Mass Transfer, 50: 1397-1407.

Liu, K.C., 2007b. Numerical analysis of dual-phase-lag heat transfer in a layered cylinder with nonlinear interface boundary conditions. Comp. Phys. Commun., 177: 307-314.

Liu, K.C., 2008. Thermal propagation analysis for living tissue with surface heating. Int. J. Thermal Sci., 47: 507-513.

Maenosono, S. and S. Saita, 2006. Theoretical assessment of FePt nanoparticles as heating elements for magnetic hyperthermia. IEEE Trans. Magnet., 42: 1638-1642.

Moroz, P., S.K. Jones and B.N. Gray, 2002. Magnetically mediated hyperthermia: Current status and future directions. Int. J. Hyperthermia, 18: 267-284.

Shirmohammadi, R., 2008. Temperature transients in spherical medium irradiated by laser pulse. Int. Commun. Heat Mass Transfer, 35: 1017-1023.

Tsuda, N., K. Kuroda and Y. Suzuki, 1996. An inverse method to optimize heating conditions in RF-capacitive hyperthermia. IEEE Trans. Biomed. Eng., 43: 1029-1037.

Virseda, P. and J.M. Pinazo, 1998. Heat conduction in multilayer spherical products by transfer functions. Int. J. Refrigerat., 21: 285-294.